Thermally and Photochemically Induced Dethreading of Fumaramide-Based Kinetically Stable Pseudo[2]rotaxanes

Alberto Martinez-Cuezva,*[a] Fatima Morales, Grace R. Marley,[a] Adrian Lopez-Lopez,[a] Juan Carlos Martinez-Costa,[a] Delia Bautista,[b] Mateo Alajarin,[a] Jose Berna*[a]

Dedicated with deep affection and respect to the memory of our friend and colleague Professor Angel Vidal

Abstract: The thermally and photochemically induced dethreading of a series of pseudo[2]rotaxanes bearing tetraalkyl substituted fumaramide axles and polyamide macrocycles is reported herein. The length of the alkyl chains at the ends of the thread, the void size and flexibility of the macrocycle and the intercomponent interactions are critical for a satisfactory dethreading process. ^{1}H NMR kinetic experiments were carried out in order to calculate the rate constants of the thermal dethreading processes and stabilities of the rotaxanes, by comparing with the similar data for the deslipping of the succinamide surrogates. The deslipping reaction occurs faster with the fumaramide systems than succinamide ones. The incorporation of adamantane moieties into the polyamide macrocycle drastically slowed down the disconnecting process. Furthermore, interlocked systems with dipropylamino groups as stoppers experienced a rapid dethreading when irradiated under UV-light, a process triggered by the fumaramide-maleamide isomerization. In this case, the *n*-propyl groups are not bulky enough to keep together both components as the number of hydrogen-bonds between thread and macrocycle is halved in the maleamide systems.

Introduction

Rotaxanes are one of the most popular systems among the diverse families of mechanically interlocked molecules.[1] Their basic structure is an axle threaded through the void of a macrocycle. The bulkiness of the stoppers located at the axle ends precludes the deslipping reaction towards the formation of the free components, maintaining the so-called mechanical bond.[2]

Kinetically stable pseudorotaxanes furnished with stoppers having a complementary size with that of the macrocycle void are prone to undergo deslipping process.[3] Thus the precise design of such terminal groups is essential to successfully build interlocked structures with a stable mechanical bond. In these cases the steric size of the stoppers is not the only parameter to have in mind. Subtle variations on the structure of the thread (flexibility, length, functional groups orientation)[4] or macrocycle (void size)[5] drastically affects on the energy necessary to break the mechanical bond. The paradigmatic example reported by Schalley nicely illustrates how a minimal hydrogen-deuterium exchange at the stoppers can notably affect to the kinetic stabilization of interlocked species.[6]

The non-covalent bonding interactions between axle and macrocycle (hydrogen bonds, aromatic stacking, etc), highly important for successfully template these systems,[7] also must be considered. The surviving of these intramolecular interactions totally depends on the environment. Changes in the temperature or polarity of the surrounding media importantly affect the stability and internal dynamics of the interlocked structures.[8] Under certain conditions the non-covalent interactions can be disrupted, triggering the dethreading of the two components when the size of the stopper is not large enough.[9] In this line we recently described an efficient protocol for the synthesis of tetralactam macrocycles through a thermal dethreading methodology from succinamide-based [2]rotaxanes.[10] The employment of a polar aprotic solvent such as DMSO, known to establish competitive intermolecular interactions with the hydrogen bond (HB) donor groups of benzylic amide rotaxanes,[11] drastically accelerates the dethreading process.

Fumaramides are well-established templates for the assembly of hydrogen-bonded rotaxanes.[12],[13] Their high efficiency (up to 97% yield) in rotaxane formation is the result of the specific preorganization of its hydrogen-bond acceptors. The reversible isomerization of fumaramides (*E* isomer) to the corresponding maleamides (*Z* isomer) carried out under different light sources or heat has been fruitfully used, for example, for controlling the internal translational movement of the macrocycle in polyamide-based interlocked structures.[13b-e,h,k,n] In fumaramide-based hydrogen-bonded [2]rotaxanes a cooperative quadruple hydrogen-bonding network is built between the binding site (fumaramide) and the macrocycle. For maleamides, only two hydrogen bonds are established between the entwined components. Thus the affinity of the macrocycle towards the two different binding sites (fumaramide *vs* maleamide) is noticeably different, allowing the control of the pirouetting rate of the ring around the thread.[13a] Light irradiation is a highly employed stimulus applied for the control of molecular machinery.[14] Jointly with fumaramide-maleamide systems,[15] azobenzene derivatives[16] or alkenes[17] have been widely employed as photoisomerizable units, among others, as components in artificial machines.

[a] Dr. A. Martinez-Cuezva, Dr. F. Morales, G. R. Marley, A. Lopez-Lopez, J. C. Martinez-Costa, Prof. Dr. M. Alajarin, Dr. J. Berna
Departamento de Química Orgánica, Facultad de Química, Regional Campus of International Excellence "Campus Mare Nostrum", Universidad de Murcia, E-30100 Murcia (Spain)
E-mail: amcuezva@um.es
ppberna@um.es
Homepage: https://qosumu.wixsite.com/socumu-lab
[b] Dr. D. Bautista
SAI, Universidad de Murcia, E-30100 Murcia (Spain)

Herein we report a complete study focused on the dethreading process of kinetically stable hydrogen-bonded pseudo[2]rotaxanes **2** and **3** bearing tetrasubstituted-fumaramide as threads (Figure 1). Two different strategies were employed for efficiently promote the disassembly of the entwined components. First, a thermal-driven dethreading was carried out and the recorded data were compared with those of the previously described succinamide-based analogues **1**. Moreover, a novel light-promoted deslipping reaction was developed. The change of the thread configuration (from fumaramide to maleamide) reducing the number of intercomponent hydrogen bonds allowed a facile dethreading even at room temperature.

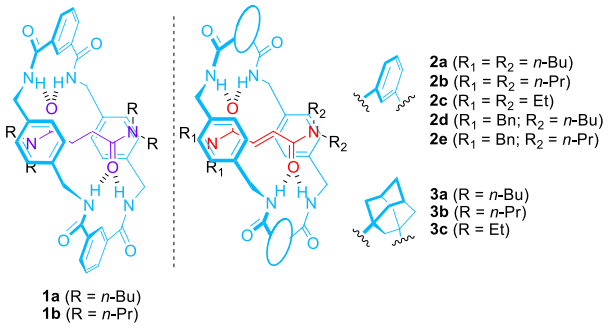

Figure 1. Interlocked systems **1-3** evaluated in this study.

Results and Discussion

Synthesis of tetraalkylsubstituted fumaramide [2]rotaxanes

In order to establish the influence of the template and the bulkiness of the alkyl chains of the stoppers (ethyl, *n*-propyl and *n*-butyl) on the stability of the mechanical bond we first prepared a series of fumaramide-based rotaxanes **2** and **3**, by employing the corresponding threads **4a-e** as binding site. Thus we reacted the threads under the standard conditions for the formation of amide-based [2]rotaxanes following a clipping methodology.[18] By using *p*-xylylenediamine and isophthaloyl chloride we were able to isolate rotaxanes **2a,b**, having *n*-butyl and *n*-propyl groups, respectively, in moderate yields (Table 1, entries 1-2).[19] Interestingly when the *N,N,N´,N´*-tetraethyl-fumaramide **4c** was used, the corresponding rotaxane **2c** was obtained in a 40% conversion, calculated by ^{1}H NMR of the reaction crude (see Supporting Information for further details, Figure S1). Moreover, the high resolution mass spectrum confirmed the presence of **2c**. Unfortunately different attempts for its isolation were unfruitful (via column chromatography or purification by precipitation/washing). Thus the size of two ethyl groups on the N atoms of the fumaramides is under the limit of the required bulkiness in order to kinetically stabilize the interlocked structure **2c**. The hydrogen-bonding interactions between the thread and the macrocycle are essential for the stabilization of the system. The existence of the interlocked structure **2c** is demonstrated, but when the formation of competitive hydrogen bonds is possible (i. e. by the presence of polar solvents, a hydrogen-bonding donor, or the use of slightly acidic silica gel in the column chromatography purification), the dissociation into the non-interlocked components is favoured. Moreover, we also synthesized rotaxanes **2d,e**, having unsymmetrical threads with two benzyl groups at one of the ends and *n*-butyl or *n*-propyl chains at the other, both obtained in reasonable moderate yields (Table 1, entries 4 and 5).

For this study we also assembled rotaxanes **3a-c**, bearing two 1,3-adamantane dicarbonyl moieties on the macrocyclic counterpart instead of the isophthaloyl functions present in **2** (Table 1, entries 6-8). The obtained yields were generally low, as a consequence of the lesser acidity of the hydrogens of the macrocyclic amides of the intermediate supramolecular complex leading to the interlocked compound.[20] The weakness of these hydrogen bonds interactions in **3a** was revealed by variable-temperature NMR experiments. These measurements led to estimate the energy barrier due to the rotation motion of the adamantane-based ring around the template giving an idea of the strength of the intercomponent interactions. When these data are compared with those obtained for rotaxane **2a**, a remarkable difference of around 5 KJ·mol^{-1} was found (see SI, Figures S3-4). As previously occurred when thread **4c** was employed, the corresponding rotaxane **3c** was formed and identified by ^{1}H NMR in the crude reaction mixture (see Figure S2), but unfortunately we were not able to isolate it.

Table 1. Synthesis of the tetrasubstituted fumaramide-based [2]rotaxanes **2-3**.[a]

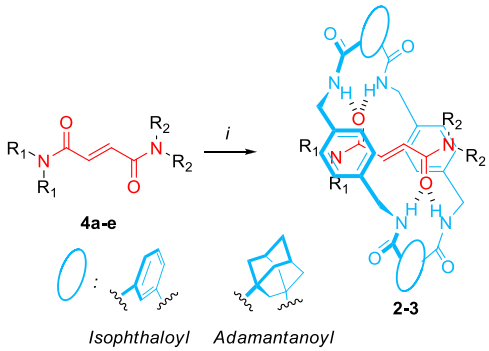

Entry	Rotaxane	R_1	R_2	Macrocycle	Yield (%)[b]
1	**2a**	*n*-Bu	*n*-Bu	Isoph	41
2	**2b**	*n*-Pr	*n*-Pr	Isoph	31
3[c]	**2c**	Et	Et	Isoph	- (42)[d]
4[e]	**2d**	Bn	*n*-Bu	Isoph	43
5	**2e**	Bn	*n*-Pr	Isoph	25
6	**3a**	*n*-Bu	*n*-Bu	Adam	7
7	**3b**	*n*-Pr	*n*-Pr	Adam	5
8[c]	**3c**	Et	Et	Adam	- (20)[d]

[a] Reaction conditions: (i) fumaramide **4**, isophthaloyl chloride or 1,3-adamantanedicarbonyl dichloride (8 equiv.), *p*-xylylenediamine (8 equiv.), Et_3N (24 equiv.), $CHCl_3$, 25 ºC, 4 h. [b] Yield of isolated product. [c] Unstable to purification via column chromatography. [d] Conversion calculated by ^{1}H NMR of the crude mixture. [e] Data from reference [13m].

Thermodynamic and kinetic parameters of the thermal dethreading process

With our interlocked systems **2** and **3** on hand we decided to study its dethreading processes under thermal conditions. Initially, we tested compounds **2** by dissolving them in a deuterated suitable solvent ($C_2D_2Cl_4$ or DMSO-d_6) and followed by ^{1}H NMR the deslippage reaction towards the formation of the free threads **4** and macrocycle **5**, with time at a constant temperature of 373 K (Scheme 1).

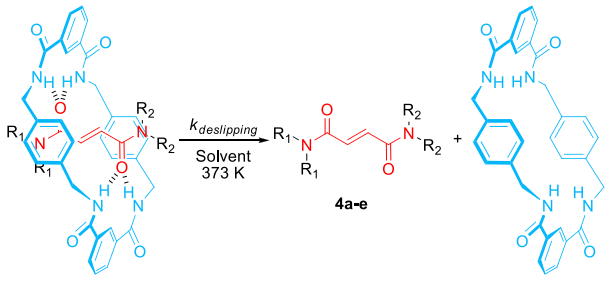

2a (R_1 = R_2 = *n*-Bu)
2b (R_1 = R_2 = *n*-Pr)
2d (R_1 = *n*-Bu; R_2 = Bn)
2e (R_1 = *n*-Pr; R_2 = Bn)

Scheme 1. Dethreading reaction of rotaxanes **2** under thermal conditions.

Next, we compared the kinetic data of fumaramide rotaxanes **2a** and **2b** with the ones previously reported by us for tetraalkyl-succinamide interlocked systems **1a,b** (Table 2, entries 1-4, and Figure 2).[10] First, we noted that the size of the stoppers of tetrabutylsubstituted 1,2-dicarboxamides rotaxanes **1a** and **2a** was bulky enough to prevent their dethreading in tetrachloroethane. In contrast, tetrapropylsubstituted 1,4-dicarboxamides derivatives **1b** and **2b** dethreaded in the same solvent by a thermal stimulus. These later ones spontaneously undergo dethreading in highly polar solvents such DMSO even at room temperature. These observations determined the solvent choice in the following NMR measurements. We also noted an important decrease of the half-life times and a subsequent increase of the deslipping constants in both rotaxanes **2** if compared with their analogous succinamide-based derivatives **1**. In early studies on the dethreading of Hunter-Vögtle anilide-based rotaxanes,[21] Schalley *et al.* reported that an increase of the flexibility of the threads led to a clear decrease of the stability of the interlocked systems, triggering their faster disassembling.[4c] The behaviour of the herein prepared systems also follows this line. The dethreading process is faster in the case of the fumaramide-based rotaxanes **2a,b**, with a better hydrogen-bonding template than the succinamide one present in **1a,b**. The minor stability of **2a,b** can be explained by the lower rotational barrier in the CO-N amide bond of the threads **4** compared with the succinamide ones, and consistent with previous studies for related tertiary amides such as disubstituted propanamides (38.5 kJ·mol^{-1}) and acrylamides (28.5 kJ·mol^{-1}) (Scheme 2).[22] The existence of a third resonance form **III** in the case of fumaramides (*N,N*-dimethylacrylamide in Scheme 2b) diminished the double-bond character of the C-N bond, enhancing its rotational motion and its flexibility (ΔΔG = 10 KJ·mol^{-1}).

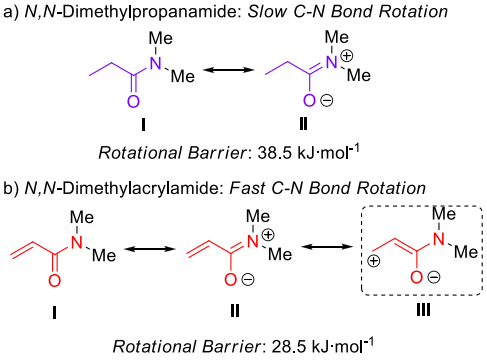

Scheme 2. Resonance forms and rotational barrier of the CO–N amide bond for: a) *N,N*-dimethylpropanamide; b) *N,N*-dimethylacrylamide.[22]

Table 2. Rate constants, half-life times and free energies for the dethreading of the rotaxanes **1** and **2** in DMSO-d_6 or $C_2D_2Cl_4$ at 373 K.

Entry	Rotaxane	Solvent	$t_{1/2}$ (h)	k x 10^5 (s^{-1})	ΔG‡ (kJ mol^{-1})[a]
1[b]	**1a**	DMSO	2.55	7.6	121.5
2	**2a**	DMSO	0.12	15.7	112.1
3[b]	**1b**	$C_2D_2Cl_4$	4.20	4.6	123.0
4	**2b**	$C_2D_2Cl_4$	0.35	55.5	115.3
5[c]	**2d**	DMSO	0.09	219.0	111.0
6	**2e**	$C_2D_2Cl_4$	0.07	273.9	110.4

[a] Gibbs free energy of activation was calculated at 373 K. [b] Data obtained from reference [10]. [c] Data obtained from reference [13m].

If we compare the behaviour of rotaxane **2a** versus **2d**, this later with an unsymmetrical thread having two benzyl groups and two butyl groups at the ends, under the same conditions, a small acceleration of the process is observed in favor of **2d** (Table 2, entries 2 and 5). A similar scenario is being played for rotaxane **2b** when compared with **2e** (Table 2, entries 4 and 6). We reasoned that the more steric-demanding benzyl groups at one end of the threads could cause steric repulsion with the macrocycle, pushing it towards the other end of the thread and, consequently, favoring the dethreading (Figure 3). Moreover, the presence of intramolecular stabilizing CH···π interactions between the alkyl chains and the aromatic groups of the macrocycle facilitates the preservation of the mechanical bond in compounds **2a,b**.[23]

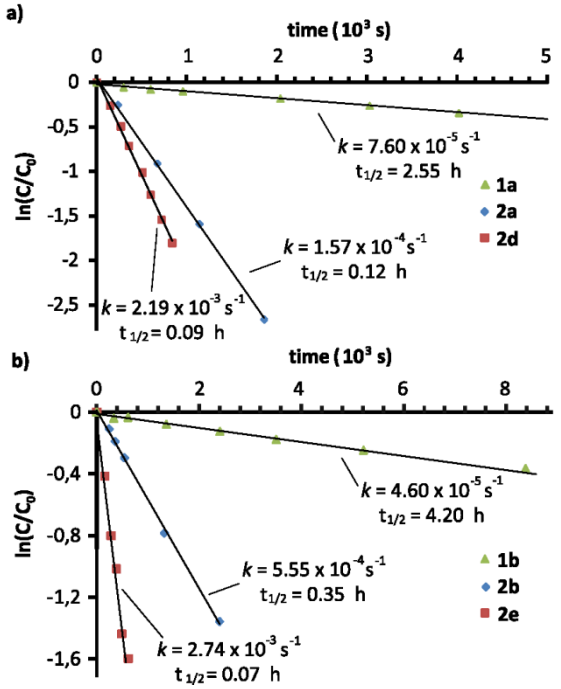

Figure 2. Dethreading of succinamide- and fumaramide-based rotaxanes: a) rotaxanes **1a**, **2a** and **2d**, having *n*-butyl groups at the threads in DMSO-d_6 at 373 K; b) rotaxanes **1b**, **2b** and **2e**, having *n*-propyl groups at the threads in $C_2D_2Cl_4$ at 373 K. Plot of ln(c/c_0) versus time for the determination of the rate constants and half-life times.

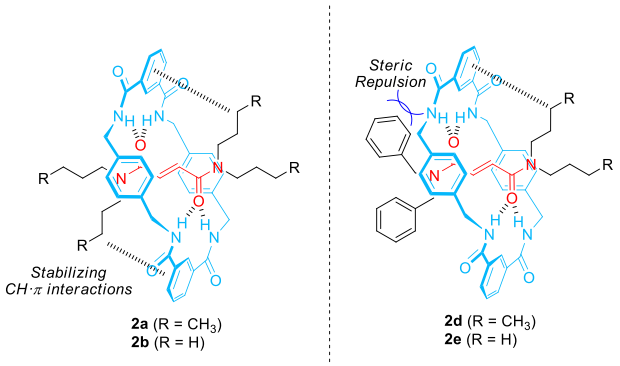

Figure 3. Intramolecular CH···π interactions and repulsive steric effects in rotaxanes **2**.

The structure of the macrocycle notably interferes on the dethreading, as previously noted in succinamide-based systems.[10] When the macrocycle incorporates two adamantane moieties, e. g. in rotaxanes **3a-b**, instead the isophthaloyl units present in compounds **2a-b**, the dethreading was slower (Table 3). The effect is remarkable when comparing rotaxanes **2a** and **3a** in DMSO at 373 K. While rotaxane **2a** can be easily separated into its two non-interlocked components (half-life time of 0.12 h), rotaxane **3a** was totally unaffected (Table 3, entries 1 and 2).[24] In the case of fumaramide rotaxanes **2b** and **3b**, with propyl groups as stoppers, the deslipping process occurred again faster when the isophthalamide moiety was present, e. i. for rotaxane **2b** (Table 3, entries 3-6). In DMSO the reaction was extremely fast, but we were able to obtain suitable data for rotaxane **3b** (Table 3, entry 4) (the deslipping rate for **2b** -entry 3- was very high precluding the data acquisition at the measurement conditions). Interestingly when compared the dethreading of **2b** and **3b** in a non-competitive solvent ($C_2D_2Cl_4$) the reaction rates were almost identical, with a higher rate for **3b**. Although the flexibility of the adamantly-based ring is larger than that of the isophthalamide one, the bulkiness of these saturated hydrocarbon core decrease the dethreading rate.

Table 3. Rate constants, half-life times and free energies for the deslipping of the rotaxanes **2a,b** and **3a-c** in DMSO-d_6 or $C_2D_2Cl_4$ at 373 K.

Entry	Rotaxane	Solvent	$t_{1/2}$ (h)	k x 10^5 (s^{-1})	$\Delta G^{\ddagger}$ (kJ mol^{-1})[a]
1	**2a**	DMSO	0.12	157.0	112.1
2[b]	**3a**	DMSO	-	-	-
3[c]	**2b**	DMSO	-	-	-
4	**3b**	DMSO	0.03	631.0	108.0
5	**2b**	$C_2D_2Cl_4$	0.35	55.4	115.3
6	**3b**	$C_2D_2Cl_4$	0.38	50.4	115.6

[a] Gibbs free energy of activation were calculated at 373 K. [b] No deslipping of **3a** was observed after 12 h. [c] The deslipping reaction finished in less than 3 min, being impossible to get the required data.

X-Ray Structures of rotaxane 3a and adamantane-based macrocycle 6

The solid state structures of rotaxane **3a** and the non-interlocked adamantane-based macrocycle **6** were obtained by single crystal X-ray diffraction analysis. The structure for **3a** clearly shows the interlocked nature of the system, with bifurcated hydrogen-bonded interactions between the two CO acceptors of the thread and the NH donors of the macrocycle (Figure 4). Moreover the macrocyclic component adopts the habitual chair conformation usually found in isophthalamide-based systems, embracing the fumaramide binding site between the two *p*-xylylene ring.

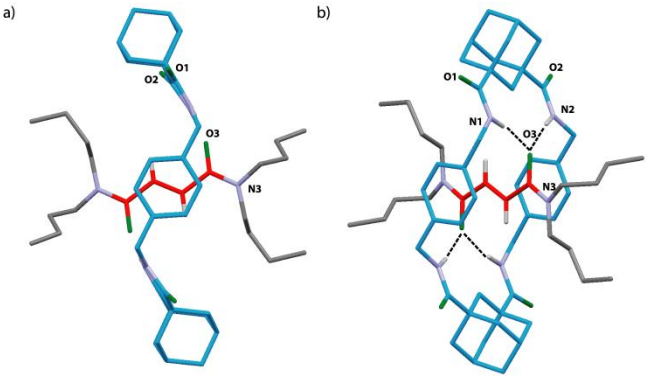

Figure 4. X-ray structure of the [2]rotaxane **3a** (CCDC 1890728): a) lateral view; b) inclined view showing the H-bond pattern. Intramolecular hydrogen bond lengths [Å] (and angles [deg]): O3HN1, 2.08 (165.4); O3HN2, 2.14 (163.7). Selected hydrogen atoms have been deleted for clarity.

The non-interlocked adamantane-based macrocycle **6** was isolated from the dethreading reaction of rotaxane **3b** and crystallized by slow cooling of a hot solution in DMF. The structure on the solid state shows that the ring adopts a highly flattened chair conformation (Figure 5). Interestingly, the aromatic *p*-xylylene rings are settled in the same average plane, contrasting with the usual face-to-face disposition in the isophthalamide-based ring[12] and the disposition displayed in the interlocked system **3a**. Moreover, the transoid and cisoid configurations of the amide bonds are alternated showing two oxygen atoms pointing the opposite face of the other two.

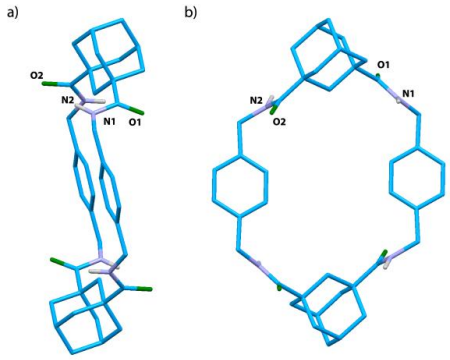

Figure 5. X-ray structure of the macrocycle **6** (CCDC 1890727): a) lateral view; b) front view. Selected hydrogen atoms have been deleted for clarity.

Photoisomerization of rotaxanes 2 and 3: Study of the kinetic stability of the *Z*-isomers.

At this point we wondered how minimizing of the number of the intramolecular hydrogen bonds in the maleamides derivatives, obtained by photoisomerizarion of systems **2** and **3**, could affect the dethreading process. We envisaged that the thermal deslippage of the maleamide-based rotaxanes *Z*-**2** and *Z*-**3** would be faster than with the corresponding interlocked fumaramides, at least in non-competitive solvents such as tetrachloroethane where the intramolecular hydrogen bonds prevail.

Thus we submitted rotaxanes **2** and **3** to light irradiation. In the case of rotaxane **2a**, with *n*-butyl groups at the ends, we were able to isolate the maleamide *Z*-**2a** (45% yield) when irradiated at 312 nm during a period of 90 min in CH_2Cl_2 at room temperature (Scheme 3) (see Supporting Information for further details).

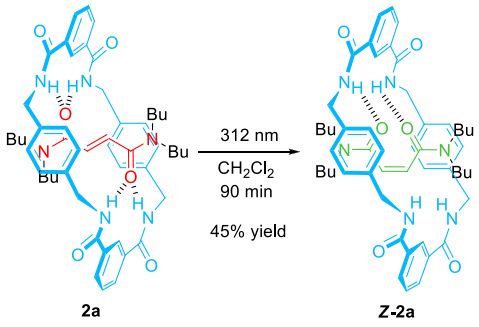

Scheme 3. Photoisomerization of rotaxane **2a** under UV light (312 nm).

With the interlocked maleamide *Z*-**2a** on hand we followed its thermal dethreading process in both DMSO-d_6 and $C_2D_2Cl_4$ as solvents, and compared the data with the fumaramide **2a** (Table 4). Whereas compound **2a** did not disassemble in $C_2D_2Cl_4$ at 373 K, its isomer *Z*-**2a** disconnect its free components *Z*-**4a** and macrocycle **5** with a dethreading rate constant of 8.66 x 10^{-5} s^{-1} ($t_{1/2}$ = 2.23 h). As it could be expected its disassembly in a highly competitive polar solvent (DMSO) occurred extremely fast, precluding the estimation of the rate constant (total disassembly in less than 5 min). Interestingly, whereas *Z*-**2a** is stable in $CDCl_3$ at room temperature after 24 h, it quickly dethreads in DMSO-d_6 (half-life time of 1.37 h) (Scheme 4). The disruption of the intercomponent hydrogen bonds in DMSO triggers the disassembly of the interlocked system.

Table 4. Rate constants, half-life times and free energies for the deslipping of the rotaxane **2a** and its isomer *Z*-**2a** in DMSO-d_6 or $C_2D_2Cl_4$ at 373 K.

Entry	Rotaxane	Solvent	$t_{1/2}$ (h)	k x 10^5 (s^{-1})	$\Delta G^{\ddagger}$ (kJ mol^{-1})[a]
1	**2a**	DMSO	0.12	157.0	112.1
2[b]	**2a**	$C_2D_2Cl_4$	-	-	-
3[c]	***Z*-2a**	DMSO	-	-	-
4[d]	***Z*-2a**	DMSO	1.37	14.2	94.9
5	***Z*-2a**	$C_2D_2Cl_4$	2.23	8.66	121.1

[a] Gibbs free energy of activation were calculated at 373 K. [b] No dethreading of **2a** was observed after 24 h. [c] The reaction finished in less than 3 min precluding the acquisition of data. [d] Reaction at 25 ºC.

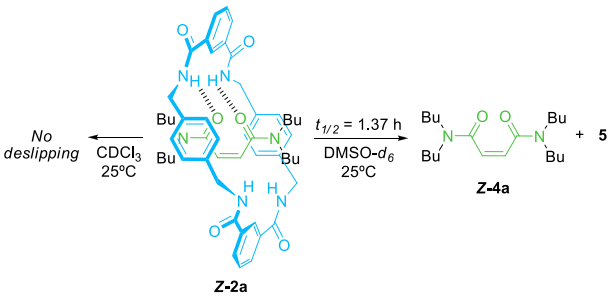

Scheme 4. Influence of the solvent polarity in the deslippage of rotaxane *Z*-**2a** at room temperature.

More interesting was the behavior of rotaxanes **2b** and **3b**, having shorter and thus, less sterically demanding *n*-propyl groups as stoppers, when submitted ~~under~~ to the same reaction conditions. Under irradiation we observed the precipitation of a white solid, corresponding to the non-interlocked macrocycles **5** or **6**, respectively (Scheme 5). The photoisomerization of the fumaramide axle of **2b** to maleamide triggered a spontaneous deslipping process, to afford the isophthalamide-based macrocycle **5** and the maleamide *Z*-**4b**. A similar behavior was observed for rotaxane **3b**, precipitating the adamantane-based macrocycle **6**. These results underline the importance of the hydrogen-bonding network between the fumaramide and the ring in the stabilization of the pseudorotaxanes. The

transformation to the maleamide reduces the strength of this hydrogen-bonding network and the dipropylamino groups are not bulky enough to preserve the entanglement of the subcomponents. The fumaramide-maleamide isomerization[24] has been fruitfully studied for the control of the translational of the macrocycle in molecular shuttles[13b-e,h,k,n] or for the acceleration of a large amplitude rotational motion,[13a] but to the best of our knowledge, this is the first time it has been explored as an input for dethreading reactions.

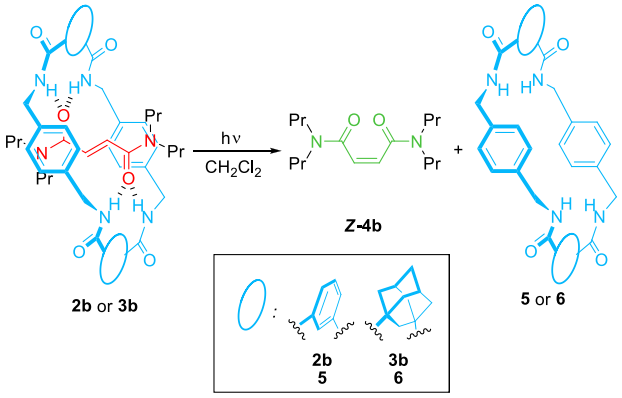

Scheme 5. Photochemically induced dethreading of rotaxanes **2b** and **3b** under UV light (254 or 312 nm).

We followed the photo-induced deslipping process over time for rotaxanes **2b**, **2e** and **3b**, bearing at least two *n*-propyl groups at one of the ends of the thread, under two different wavelengths (254 nm and 312 nm) (see Supporting Information for further details). Figure 6 shows the deslipping reaction of rotaxane **2b** with time (up to 60 min), when irradiated at 312 nm. Signals related to hydrogen atoms of the rotaxane **2b** (in blue, red and black) decreased with time, whereas signals attributed to the maleamide-based thread *Z*-**4b** (in green) increased. Signals corresponding to the free macrocycle **5** are not observed due to its insolubility in $CDCl_3$ (see Insets in Figure 6).

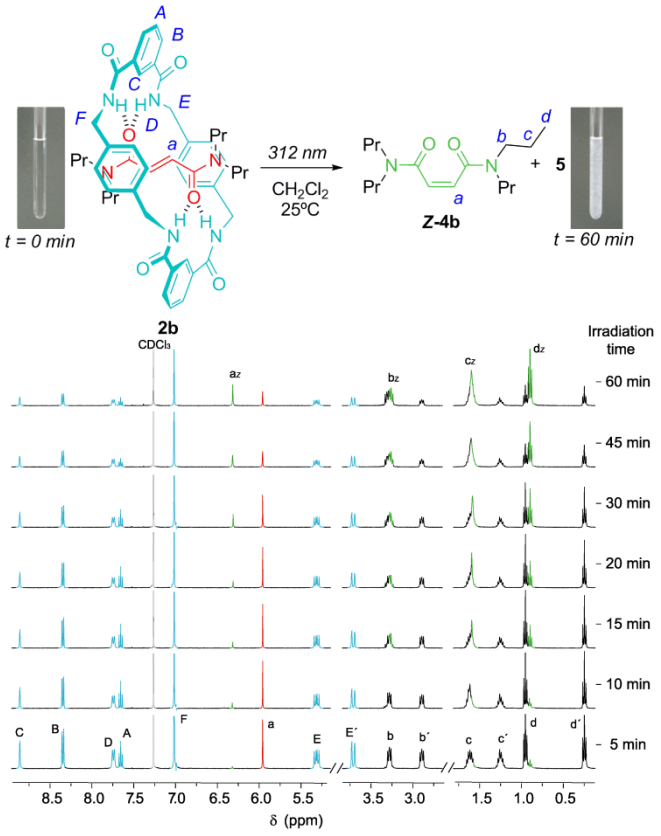

Figure 6. Stack plot of partial ^{1}H NMR spectra ($CDCl_3$, 298 K) of the photo-induced dethreading of **2b** over time. Capital letters A-F correspond to the hydrogen atoms of the macrocycle (in light blue) and lowercase letters a-d correspond to the hydrogen atoms of **2b** (in red and black) and the free maleamide ***Z*-4b** (in green). Insets: NMR tubes containing samples of the reaction at time = 0 min and time = 60 min, where a white precipitate (macrocycle **5**) appeared.

The photo-induced deslipping process is a unimolecular reaction, and, consequently, it should follow first order kinetics (Figure 7).[26],[27] Thus, the integration of the different signals allowed us to obtain the kinetic data for these transformations (Table 5). The deslipping of **2b** is more rapid when irradiating at a higher energy wavelength (254 nm vs 312 nm) (Figure 7a, Table 5, entries 1 and 2). This behavior is general for the rest of the systems **2e** and **3b** (Table 5, entries 3-4 and 5-6). When 312 nm lamps were used, only the presence of the isomerized thread *Z*-**4b** or *Z*-**4e** was observed in the reaction media. In contrast, an increasing amount of *E*-**4b** and *E*-**4e** was also identified under irradiation at 254 nm, until the photostationary equilibrium was reached, together with the formation of byproducts after long periods of time. Interestingly, the isomerization of the free thread **4b** into its isomeric *Z*-**4b**, which was obtained in full conversion when irradiated at 312 nm, was faster than in the case of the corresponding rotaxanes (Figure 7b). Most probably, the presence of the interlocked macrocycle counterpart, with aromatic groups in their structure, absorbed part of the irradiated light, decreasing the isomerization rate of the fumaramide double bond. Additionally, the establishment of intramolecular hydrogen-bonded interactions between the thread and the macrocycle could also contribute to the slower reaction rate.[28]

Table 5. Rate constants, half-life times and free energies for the deslippage of the rotaxanes **2b**, **2e** and **3b** under UV-light irradiation at 298 K. Isomerization of thread **4b**.

Entry	Compound	UV source (nm)	$t_{1/2}$ (h)	k x 10^5 (s^{-1})	$\Delta G^{\ddagger}$ (kJ mol^{-1})[a]
1	**2b**	312	0.79	24.8	93.6
2[b]	**2b**	254	0.18	107.0	89.9
3	**2e**	312	0.58	32.9	92.9
4[b]	**2e**	254	0.34	56.3	91.5
5	**3b**	312	0.72	26.6	93.4
6[b]	**3b**	254	0.62	31.3	93.0
7	**4b**	312	0.16	117.0	89.7
8[c]	**4b**	254	-	-	-

[a] Gibbs free energies of activation were calculated at 373 K. [b] An increasing amount of *E*-**4b** or *E*-**4e** was observed with time. [c] The reaction could not be followed since a photostationary state is established.

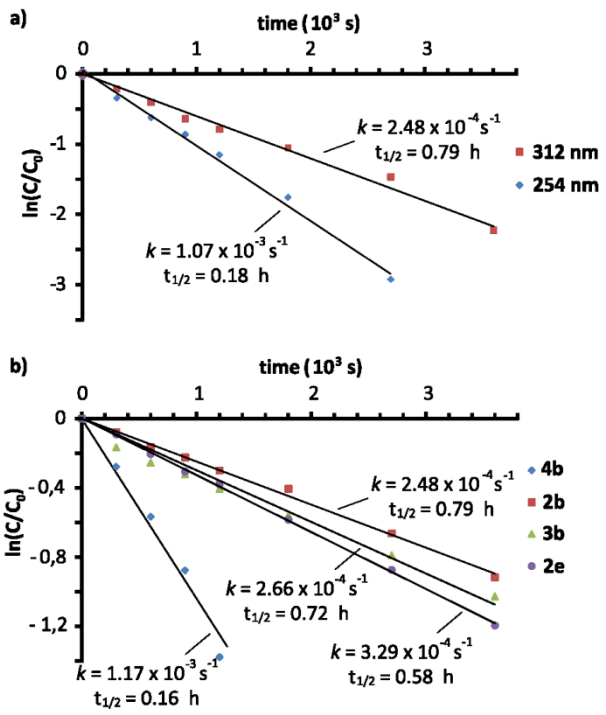

Figure 7. Photochemically induced dethreading process. Plot of $\ln(c/c_0)$ versus time for the determination of the rate constants and half-life times.of: a) rotaxane **2b** at 312 nm and 254 nm; b) rotaxanes **2b, 2e** and **3b**, with the isomerization reaction of **4b** at 312 nm.

Conclusions

In summary we have synthesized a series of kinetically stable fumaramide-based [2]pseudorotaxanes by varying the length of the stoppers present at the ends of the threads in order to preserve the mechanical bond. We have found that the propyl groups are the smallest ones that can stabilize it. The dethreading of fumaramide-based pseudorotaxanes under thermal conditions was found to be easier than that of their corresponding succinamide-based surrogates, due to the higher mobility of their dialkylamino stoppers. Moreover, a photo-induced dethreading process of these olefin assemblies has also been developed. The light-triggered isomerization of the interlocked fumaramides, having dipropylamino stoppers, forms the corresponding maleamides which spontaneous dethreaded into their components. The change from the quadruple hydrogen-bonding pattern in the fumaramide-based systems to a weaker one in the maleamide derivatives, with only two possible hydrogen bonds, is enough to break the interlocked structure. All these findings could play a relevant role in the design of novel supramolecular catalysts and functional photoresponsive host-guest systems.

Experimental Section

General Methods. All reagents were purchased from commercial suppliers and used without further purification. HPLC grade solvents were dried in a solvent purification system by passing it through an activated alumina column before use. Column chromatography was carried out using silica gel (60 Å, 70-200 μm) as stationary phase, and TLC was performed on precoated silica gel on aluminium cards (0.25 mm thick, with fluorescent indicator 254 nm) and observed under UV light. All melting points were determined on a Kofler hot-plate melting point apparatus and are uncorrected. ^{1}H- and ^{13}C-NMR spectra were recorded at 298 K on 300 and 400 MHz spectrometers. ^{1}H NMR chemical shifts are reported relative to Me_4Si and were referenced via residual proton resonances of the corresponding deuterated solvent whereas ^{13}C NMR spectra are reported relative to Me_4Si using the carbon signals of the deuterated solvent. Abbreviations of coupling patterns are as follows: br, broad; s, singlet; d, doublet; t, triplet; q, quadruplet; m, multiplet. Coupling constants (*J*) are expressed in Hz. High resolution mass spectra (HRMS) were obtained using a time-of-flight (TOF) instrument equipped with electrospray ionization (ESI). The irradiation experiments were carried out in quartz tubes in a photoreactor Luzchem LZC-4V under 254 nm (62 $W \cdot m^{-2}$) and 312 nm (56 $W \cdot m^{-2}$).

Materials. Threads **4a-c**[29] and **4d**[13m] and rotaxane **2d**[13m] were prepared as previously reported.

Synthesis of thread 4e. To a stirred solution of (*E*)-4-(dibenzylamino)-4-oxobut-2-enoic acid[29] (2.00 g, 6.78 mmol) in anhydrous CH_2Cl_2 (50 mL) was added dipropylamine (1.10 mL, 8.14 mmol), HOBt (915 mg, 6.78 mmol) and DMAP (82 mg, 0.68 mmol). The reaction mixture was cooled to 0ºC and DCC (1.40g, 6.78 mmol) was added. After 30 min, the reaction was warmed to room temperature and was stirred for 24 h. After this time the resulting suspension was filtered and the filtrate was washed with an aqueous solution of 1M HCl (2 x 30 mL), saturated $NaHCO_3$ (2 x 30 mL) and brine (2 x 30 mL). The organic phase was dried over anhydrous $MgSO_4$ and concentrated under reduced pressure. The resulting residue was subjected to column chromatography (silica gel) using a mixture of hexane/AcOEt (3/1). The solvent was removed under reduced pressure to give the title product as a yellow oil (**4e**, 2.10 g, 82 %); ^{1}H NMR (400 MHz, $CDCl_3$, 298 K) δ = 7.51 (d, *J*= 14.6 Hz, 1H), 7.46 (d, *J*= 14.6 Hz, 1H), 7.37-7.22 (m, 8H), 7.18-7.13 (m, 2H), 4.66 (s, 2H), 5.51 (s, 2H), 3.37-3.30 (m, 4H), 1.68-1.52 (m, 4H), 0.93 (t, *J*= 7.3 Hz, 1H), 0.83 (t, *J*= 7.4 Hz, 1H); ^{13}C NMR (101 MHz, $CDCl_3$, 298 K) δ = 166.1 (CO), 164.7 (CO), 136.9 (C), 136.1 (C), 132.9 (CH), 131.0 (CH), 129.0 (CH), 128.8 (CH), 128.4 (CH), 127.9 (CH), 127.7 (CH), 126.8 (CH), 50.2 (CH_2), 50.0 (CH_2), 48.7 (CH_2), 48.6 (CH_2), 23.1 (CH_2), 21.0 (CH_2), 11.5 (CH_3), 11.2 (CH_3); HRMS (ESI) calcd for $C_{24}H_{31}N_2O_2$ [M + H]$^+$ 379.2380, found 379.2387.

General procedure for the synthesis of the [2]rotaxanes 2a-e and 3a-b. The thread (1 equiv.) and Et_3N (24 equiv.) in anhydrous $CHCl_3$ (300 mL) were stirred vigorously while solutions of *p*-xylylenediamine (8 equiv.) in anhydrous $CHCl_3$ (20 mL) and the corresponding acid dichloride (8 equiv.) in anhydrous $CHCl_3$ (20 mL) were simultaneously added over a period of 4 h using motor-driven syringe pumps. After a further 4 h, the resulting suspension was filtered through a Celite pad and washed with water (2 x 50 mL), a solution of HCl 1M (2 x 50 mL), a saturated solution of $NaHCO_3$ (2 x 50 mL) and brine (2 x 50 mL). The organic phase was then dried over $MgSO_4$, and the solvent was removed under reduced pressure. The resulting solid was subjected to column chromatography (silica gel) to yield unconsumed thread and [2]rotaxane.

Rotaxane **2a** was obtained using the described method from thread **4a** (0.50 g, 1.48 mmol). The resulting residue was subjected to column chromatography (silica gel) using a $CHCl_3$/MeOH (40/1) mixture. The solvent was removed under reduced pressure to give the title product as a white solid (682 mg, 53%); mp > 300 ºC (decomp.); ^{1}H NMR (3.00 MHz, $CDCl_3$): δ = 8.86 (s, 2H), 8.32 (dd, 4H, *J* = 7.8, 0.9 Hz), 7.75 (d, 4H, *J* = 8.3 Hz), 7.64 (t, 2H, *J* = 7.8 Hz), 7.00 (s, 8H), 5.97 (s, 2H), 5.27 (dd, 4H, *J* = 14.2, 9.1 Hz), 3.71 (dd, 4H, *J* = 14.2, 1.2 Hz), 3.35-3.25 (m, 4H), 2.96-2.88 (m, 4H), 1.62-1.48 (m, 4H), 1.38-1.14 (m, 8H), 0.92 (t, 6H, *J* = 7.3 Hz), 0.68-0.48 (m, 10H) ppm. ^{13}C NMR (75 MHz, $CDCl_3$): δ = 165.5 (CO), 165.2 (CO), 138.2 (C), 133.4 (C), 132.3 (CH), 129.6 (CH), 129.1 (CH), 128.4 (CH), 122.8 (CH), 49.1 (CH_2), 48.0 (CH_2), 43.5 (CH_2), 32.3 (CH_2), 30.2 (CH_2), 20.3 (CH_2), 19.8 (CH_2), 13.9 (CH_3), 13.7 (CH_3) ppm. HRMS (ESI+) m/z calcd for $C_{52}H_{67}N_6O_6$ $[M + H]^+$ 871.5117, found 871.5123.

Rotaxane **2b** was obtained using the described method from thread **4b** (0.50 g, 1.77 mmol). The resulting residue was subjected to column chromatography (silica gel) using a $CHCl_3$/MeOH (40/1) mixture. The solvent was removed under reduced pressure to give the title product as a white solid (446 mg, 31%); mp 262-264 ºC; ^{1}H NMR (300 MHz, $CDCl_3$): δ = 8.86 (s, 2H), 8.35 (d, *J*= 7.7 Hz, 4H), 7.76-7.63 (m, 6H), 7.01 (s, 8H), 5.95 (s, 2H), 5.35-5.27 (dd, *J*= 14.1, 9.3 Hz, 4H), 3.71 (d, *J*= 14.1 Hz, 4H), 3.35-3.20 (m, 4H), 2.95-2.85 (m, 4H), 1.70-1.55 (m, 4H), 1.30-1.20 (m, 4H), 0.95 (t, *J*= 7.3 Hz, 6H), 0.24 (t, *J*= 7.2 Hz, 6H). ^{13}C NMR (75 MHz, $CDCl_3$): δ = 165.5 (CO), 165.3 (CO), 138.3 (C), 133.5 (C), 132.3 (CH), 129.8 (CH), 129.0 (CH), 128.4 (CH), 122.7 (CH), 50.9 (CH_2), 50.1 (CH_2), 43.4 (CH_2), 31.1 (CH_2), 23.5 (CH_2), 21.4 (CH_2), 11.8 (CH_3), 10.5 (CH_3) ppm. HRMS (ESI+) m/z calcd for $C_{48}H_{59}N_6O_6$ $[M + H]^+$ 815.0107; found: 815.0109.

Rotaxane **2e** was obtained by using the previously described method from thread **4b** (0.50 g, 1.32 mmol). The crude product was subjected to column chromatography on silica gel using a $CHCl_3$/MeOH (40/1) mixture, to give the title product as a white solid (303 mg, 25%). mp 265-267 ºC; ^{1}H NMR (300 MHz, $CDCl_3$, 298 K) δ = 8.81 (s, 1H), 8.51 (s, 1H), 8.39 (d, *J*= 7.6 Hz, 2H), 8.20 (d, *J*= 7.7 Hz, 2H), 7.69 (t, *J*= 7.7 Hz, 1H), 7.63-7.43 (m, 5H), 7.42-7.36 (m, 5H), 7.24-7.06 (m, 3H), 6.91-6.76 (m, 10H), 6.02 (d, *J*= 14.5 Hz, 1H), 5.96 (d, *J*= 14.5 Hz, 1H), 5.30-5.05 (m, 4H), 4.57 (s, 2H), 4.35 (s, 2H), 3.71 (d, *J*= 13.9 Hz, 2H), 3.45 (d, *J*= 13.9 Hz, 2H), 3.22-3.13 (m, 2H), 2.88-2.79 (m, 2H), 1.62-1.46 (m, 2H), 1.27-1.14 (m, 2H), 0.86 (t, *J*= 7.4 Hz, 3H), 0.19 (t, *J*= 7.4 Hz, 3H); ^{13}C NMR (75 MHz, $CDCl_3$, 298 K) δ = 166.5 (CO), 165.5 (CO), 165.4 (CO), 164.8 (CO), 138.1 (C), 138.0 (C), 135.9 (C), 134.6 (C), 133.6 (C), 133.2 (C), 132.6 (CH), 132.0 (CH), 130.0 (CH), 129.9 (CH), 129.4 (CH), 129.2 (CH), 129.0 (CH), 128.9 (CH), 128.9 (CH), 128.5 (CH), 125.9 (CH), 122.8 (CH), 122.1 (CH), 51.8 (CH_2), 51.6 (CH_2), 50.9 (CH_2), 50.2 (CH_2), 43.6 (CH_2) , 43.2 (CH_2), 23.6 (CH_2), 21.3 (CH_2), 11.7 (CH_3), 10.4 (CH_3); HRMS (ESI) calcd for $C_{56}H_{59}N_6O_6$ $[M + H]^+$ 911.4491, found 911.4474.

Rotaxane **3a** was obtained using the described method from thread **4a** (950 mg, 2.79 mmol). The resulting residue was subjected to column chromatography (silica gel) using a $CHCl_3$/MeOH (98/2) mixture. The solvent was removed under reduced pressure to give the title product as a white solid (192 mg, 7%); mp > 250 ºC; ^{1}H NMR (400 MHz, $CDCl_3$): δ = 7.09 (d, *J* = 9.1 Hz, 4H), 6.90 (s, 8H), 5.84 (s, 2H), 4.92-4.87 (m, 4H), 3.60 (d, *J* = 14.1 Hz, 4H), 3.35-3.31 (m, 4H), 3.17-3.13 (m, 4H), 2.68-2.60 (m, 2H), 2.31-2.10 (m, 12H), 1.85-1.82 (m, 4H), 1.69-1.54 (m, 18H), 1.44-1.33 (m, 8H), 1.04-0.99 (m, 12H) ppm. ^{13}C NMR (100 MHz, $CDCl_3$): δ = 177.6 (CO), 164.8 (CO), 137.7 (C), 129.1 (C), 127.4 (CH), 48.8 (CH_2), 48.0 (CH_2), 43.6 (CH_2), 41.7 (CH_2), 39.7 (CH_2), 38.7 (CH_2), 35.3 (CH_2), 32.5 (CH_2), 30.0 (CH_2), 28.2 (CH), 20.7 (CH_2), 20.6 (CH_2), 14.2 (CH_2), 14.0 (CH_3) ppm. HRMS (ESI+) m/z calcd for $C_{59}H_{83}N_6O_6$ $[M + H]^+$ 987.6609, found 987.6673.

Rotaxane **3b** was obtained using the described method from thread **4b** (788 mg, 2.8 mmol). The resulting residue was subjected to column chromatography (silica gel) using a $CHCl_3$/AcOEt (3/1) mixture. The solvent was removed under reduced pressure to give the title product as a white solid (130 mg, 5%); mp > 250 ºC; ^{1}H NMR (400 MHz, $CDCl_3$): δ = 7.09 (d, *J* = 9.7 Hz, 4H), 6.89 (s, 8H), 5.80 (s, 2H), 4.95-4.89 (m, 4H), 3.55 (d, *J* = 14.1 Hz, 4H), 3.31-3.27 (m, 4H), 3.14-3.10 (m, 4H), 2.62-2.54 (m, 2H), 2.29-2.10 (m, 12H), 1.86-1.81 (m, 6H), 1.69-1.56 (m, 16H), 1.02-0.99 (m, 12H) ppm. ^{13}C NMR (100 MHz, $CDCl_3$): δ = 177.6 (CO), 164.9 (CO), 137.8 (C), 129.1 (CH), 127.5 (CH), 50.6 (CH_2), 50.2 (CH_2), 43.5 (CH_2), 41.7 (CH_2), 39.6 (CH_2), 38.7 (CH_2), 35.3 (CH_2), 28.4 (CH), 23.4 (CH_2), 21.3 (CH_2), 12.0 (CH_3) ppm. HRMS (ESI+) m/z calcd for $C_{55}H_{75}N_6O_6$ $[M + H]^+$ 931.5983, found 931.6052.

Dethreading of [2]rotaxane *Z*-2a for the isolation of thread *Z*-4a. A solution of rotaxane ***Z*-2a** (50 mg, 0.057 mmol) in DMSO (1 mL) was stirred at 100 ºC for 15 min. After this time Et_2O (5 mL) was added and the mixture was washed with brine (4 x 20 mL). The solvent was removed under reduced pressure. The resulting residue was subjected to column chromatography (silica gel) using a hexane/AcOEt (3/1) mixture to give the title product as a yellow oil (18 mg, 95%); ^{1}H NMR (400 MHz, $CDCl_3$): δ = 6.28 (s, 2H), 3.35-3.25 (m, 8H), 1.60-1.50 (m, 8H), 1.35-1.25 (m, 8H), 0.95-0.88 (m, 12H) ppm. ^{13}C NMR (100 MHz, $CDCl_3$): δ = 166.5 (CO), 129.3 (CH), 48.4 (CH_2), 45.2 (CH_2), 31.2 (CH_2), 29.8 (CH_2), 20.4 (CH_2), 20.2 (CH_2), 14.0 (CH_3), 13.9 (CH_3) ppm. HRMS (ESI+) m/z calcd for $C_{20}H_{39}N_2O_2$ $[M + H]^+$ 339.3006, found 339.3012.

Irradiation of [2]rotaxanes 2b, 2e and 3b under UV light. Isolation of threads *Z*-4b and *Z*-4e and the adamantane-based macrocycle 6.

A solution of the corresponding rotaxane **2b**, **2e** or **3b** (0.025 mmol) in CH_2Cl_2 (40 mL) was placed in a quartz vessel under N_2 atm. The solution was irradiated under UV light (312 or 254 nm) during 90 min. Different aliquots (5 mL) were taken at different times (5, 10, 15, 20, 30, 45, 60 and 90 min) and the conversion towards the formation of threads *Z*-**4b** and *Z*-**4e** analyzed by ^{1}H NMR. The corresponding *Z* threads and macrocycle **6** were isolated from the reaction media either by column chromatography or filtration (for macrocycle 6).

Z-**4b** was obtained using the described method from rotaxane **2b** (40 mg, 0.050 mmol) after 90 min of irradiation at 312 nm. The resulting reaction mixture was subjected to column chromatography (silica gel) using a hexane/AcOEt (3/1) mixture. The solvent was removed under reduced pressure to give the title product as yellow oil (10.58 mg, 75%); ^{1}H NMR (400 MHz, $CDCl_3$): δ = 6.30 (s, 2H), 3.31-3.21 (m, 8H), 1.64-1.52 (m, 8H), 0.87 (t, *J* = 12 Hz, 12H) ppm. ^{13}C NMR (100 MHz, $CDCl_3$): δ = 166.6 (CO), 129.4 (C), 50.3 (CH_2), 47.1 (CH_2), 22.3 (CH_2), 20.9 (CH_2), 11.5 (CH_3), 11.4 (CH_3) ppm. HRMS (ESI+) m/z calcd for $C_{16}H_{31}N_2O_2$ $[M + H]^+$ 283.2380, found 283.2377.

Z-**4e** was obtained using the described method from rotaxane **2e** (50 mg, 0.055 mmol) after 90 min of irradiation at 312 nm. The resulting reaction mixture was subjected to column chromatography (silica gel) using a hexane/AcOEt (3/1) mixture. The solvent was removed under reduced pressure to give the title product as yellow oil (16.61 mg, 80%); ^{1}H NMR (400 MHz, $CDCl_3$): δ = 7.37-7.20 (m, 10H), 6.44-6.37 (m, 2H), 4.61 (s, 2H'), 4.49 (s, 2H), 3.39-3.24 (m, 4H), 1.70-1.59 (m, 4H), 0.96-0.89 (m, 6H) ppm. ^{13}C NMR (100 MHz, $CDCl_3$): δ = 167.7 (CO), 166.4 (CO), 136.9

(C), 136.6 (C), 130.5 (CH), 129.3 (CH), 129.0 (CH), 128.7 (CH), 128.6 (CH), 127.7 (CH), 127.4 (CH), 127.2 (CH), 50.8 (CH_2), 50.3 (CH_2), 47.5 (CH_2), 47.2 (CH_2), 22.4 (CH_2), 20.9 (CH_2), 11.6 (CH_3), 11.4 (CH_3) ppm. HRMS (ESI) calcd for $C_{24}H_{31}N_2O_2$ $[M + H]^+$ 379.2380, found 379.2371.

Macrocycle **6** was obtained by filtration of the reaction media after irradiation for 90 min under 312 nm, starting from rotaxane **3b** (50 mg, 0.053 mmol). The solid residue was washed with ether and pentane, to give the title product as a white solid (27.5 mg, 79%); mp > 300 ºC; ^{1}H NMR (400 MHz, $CDCl_3$): δ = 7.17 (s, 8H), 5.93 (t, *J* = 5.8 Hz, 4H), 4.39 (d, *J* = 5.8 Hz, 8H), 2.21-2.25 (m, 4H), 1.80-2.00 (m, 17H), 1.72-1.75 (m, 3H), ppm. ^{13}C NMR (100 MHz, DMSO-d_6, 373K): δ = 175.7 (CO), 137.8 (C), 126.5 (CH), 41.5 (CH_2), 40.4 (C), 37.6 (CH_2), 34.9 (CH_2), 27.5 (CH) ppm. HRMS (ESI+) m/z calcd for $C_{40}H_{48}N_4O_4$ $[M + H]^+$ 649.3748, found 649.3676.

Acknowledgments

This work was supported by the MINECO (CTQ2017-87231-P) with joint financing by FEDER Funds from the European Union, and Fundacion Seneca-CARM (Project 20811/PI/18). A. M.-C. thanks Ministerio de Ciencia, Innovación y Universidades for his Ramon y Cajal contract (RYC-2017-22700). F. M. thanks Fundación Séneca for her Saavedra Fajardo postdoctoral contract and funding (20025/SF/16).

Keywords: Fumaramides • Rotaxanes • Supramolecular chemistry • Dethreading kinetics • Photoisomerization

[1] a) G. Schill in *Catenanes, Rotaxanes and Knots*, Academic Press, New York, **1971**; b) *Molecular Catenanes, Rotaxanes, and Knots,* Eds. J. P. Sauvage, C. Dietrich-Buchecker, Wiley-VCH, Weinheim, **1999**.

[2] C. J. Bruns, J. F. Stoddart in *The Nature of the Mechanical Bond: From Molecules to Machines*, Wiley, New York, **2016**.

[3] a) M. Asakawa, P. R. Ashton, R. Ballardini, V. Balzani, M. Bělohradský, M. T. Gandolfi, O. Kocian, L. Prodi, F. M. Raymo, J. F. Stoddart, M. Venturi, *J. Am. Chem. Soc*. **1997**, *119*, 302–310; b) P. R. Ashton, I. Baxter, M. C. T. Fyfe, F. M. Raymo, N. Spencer, J. F. Stoddart, A. J. P. White, D. J. Williams, *J. Am. Chem. Soc.* **1998**, *120*, 2297–2307.

[4] a) G. M. Hübner, G. Nachtsheim, Q. Y. Li, C. Seel, F. Vögtle, *Angew. Chem. Int. Ed*. **2000**, *39*, 1269–1272; b) A. Affeld, G. M. Hübner, C. Seel, C. A. Schalley, *Eur. J. Org. Chem.* **2001**, 2877–2890; c) P. Linnartz, S. Bitter, C. A. Schalley, *Eur. J. Org. Chem.* **2003**, 4819–4829; d) P. Linnartz, C. A. Schalley, *Supramol. Chem.* **2004**, *16*, 263–267.

[5] C. Heim, A. Affeld, M. Nieger, F. Vögtle, *Helv. Chim. Acta* **1999**, *82*, 746–759.

[6] T. Felder, C. A. Schalley, *Angew. Chem. Int. Ed*. **2003**, *42*, 2258–2260.

[7] *From Non-Covalent Assemblies to Molecular Machines* (Eds.: J.-P. Sauvage, P. Gaspard), Wiley-VCH, Weinheim, **2011**.

[8] a) A. M. Rijs, N. Sändig, M. N. Blom, J. Oomens, J. S. Hannam, D. A. Leigh, F. Zerbetto, W. J. Buma, *Angew. Chem. Int. Ed*. **2010**, *49*, 3896–3900; b) M. R. Panman, B. H. Bakker, D. den Uyl, E. R. Kay, D. A. Leigh, W. Jan Buma, A. M. Brouwer, J. A. J. Geenevasen, S. Woutersen, *Nature Chem.* **2013**, *5*, 929–934.

[9] a) Y. Tachibana, N. Kihara, Y. Furusho, T. Takata, *Org. Lett.* **2004**, *6*, 4507–4509; b) Y. Suzaki, A. Takagi, K. Osakada, *Chem. Lett*. **2010**, *39*, 510–512.

[10] A. Martinez-Cuezva, L. V. Rodrigues, C. Navarro, F. Carro-Guillen, L. Buriol, C. P. Frizzo, M. A. P. Martins, M. Alajarin, J. Berna, *J. Org. Chem.* **2015**, *80*, 10049–10059.

[11] A. S. Lane, D. A. Leigh, A. Murphy, *J. Am. Chem. Soc*. **1997**, *119*, 11092–11093.

[12] F. G. Gatti, D. A. Leigh, S. A. Nepogodiev, A. M. Z. Slawin, S. J. Teat, J. K. Y. Wong, *J. Am. Chem. Soc*. **2001**, *123*, 5983–5989.

[13] a) F. G. Gatti, S. León, J. K. Y. Wong, G. Bottari, A. Altieri, M. A. F. Morales, S. J. Teat, C. Frochot, D. A. Leigh, A. M. Brouwer, F. Zerbetto, *Proc. Natl. Acad. Sci. U. S. A.* **2003**, 100, 10–14; b) A. Altieri, G. Bottari, F. Dehez, D. A. Leigh, J. K. Y. Wong, F. Zerbetto, *Angew. Chem. Int. Ed*. **2003**, 42, 2296–2300; c) G. Bottari, F. Dehez, D. A. Leigh, P. J. Nash, E. M. Perez, J. K. Y.Wong, F. Zerbetto, *Angew. Chem. Int. Ed*. **2003**, *42*, 5886–5889; d) G. Bottari, D. A. Leigh, E. M. Perez, *J. Am. Chem. Soc.* **2003**, 125, 13360–13361; e) E. M. Perez, D. T. F. Dryden, D. A. Leigh, G. Teobaldi, F. Zerbetto, *J. Am. Chem. Soc*. **2004**, *126*, 12210–12211; f) A. Mateo-Alonso, G. M. A. Rahman, C. Ehli, D. M. Guldi, G. Fioravanti, M. Marcaccio, F. Paolucci, M. Prato, *Photochem. Photobiol. Sci.* **2006**, 5, 1173–1176; g) A. Mateo-Alonso, A. M. Prato, *Tetrahedron* **2006**, 62, 2003–2007; h) M. Alvarez-Perez, S. M. Goldup, D. A. Leigh, A. M. Z. Slawin, J. Am. Chem. Soc. **2008**, 130, 1836; i) F. Y. Ji, L. L. Zhu, X. Ma, Q. C. Wang, H. Tian, *Tetrahedron Lett.* **2009**, 50, 597–600; j) N. S. Simpkins, D. F. Weske, L. Male, S. J. Coles, M. B. Pitak, *Chem. Commun*. **2013**, 49, 5010–5012; k) A. Martinez-Cuezva, S. Valero-Moya, M. Alajarin, J. Berna, *Chem. Commun.* **2015**, *51*, 14501–14504; l) P. Liu, X. Shao, C. Chipot, W. Cai, *Chem. Sci.* **2016**, *7*, 457–462; m) A. Martinez-Cuezva, C. Lopez-Leonardo, D. Bautista, M. Alajarin, J. Berna, *J. Am. Chem. Soc.* **2016**, *138*, 8726–8729; n) A. Martinez-Cuezva, A. Saura-Sanmartin, T. Nicolas-Garcia, C. Navarro, R.-A. Orenes, M. Alajarin, J. Berna, *Chem. Sci*. **2017**, *8*, 3775–3780; o) A. Martinez-Cuezva, D. Bautista, M. Alajarin, J. Berna, *Angew. Chem. Int. Ed*. **2018**, *57*, 6563–6567.

[14] a) S. Saha, J. F. Stoddart, *Chem. Soc. Rev*. **2007**, *36*, 77–92; b) V. Balzani, A. Credi, M. Venturi, *Chem. Soc. Rev.* **2009**, *38*, 1542–1550; c) J. M. Abendroth, O. S. Bushuyev, P. S. Weiss, C. J. Barrett, *ACS Nano*, **2015**, *9*, 7746–7768; d) L. Wang, Q. Li, *Chem. Soc. Rev*. **2018**, *47*, 1044–1097.

[15] a) J. Berná, D. A. Leigh, M. Lubomska, S. M. Mendoza, E. M. Pérez, P. Rudolf, G. Teobaldi, F. Zerbetto, *Nature Mater*, **2005**, *4*, 704–710; b) V. Balzani, A. Credi, M. Venturi, *Chem. Soc. Rev.* **2009**, *38*, 1542–1550; c) S. Silvi, M. Venturi, A. Credi, *Chem. Commun*. **2011**, *47*, 2483–2489.

[16] K. R. Sunil Kumar, T. Kamei, T. Fukaminato, N. Tamaoki, *ACS Nano*, **2014**, *8*, 4157–4165

[17] a) N. Koumura, R. W. J. Zijlstra, R. A. van Delden, N. Harada, B. L. Feringa, *Nature*, **1999**, *401*, 152–155; b) R. Eelkema, M. M. Pollard, J. Vicario, N. Katsonis, B. S. Ramon, C. W. M. Bastiaansen, D. J. Broer, B. L. Feringa, *Nature*, **2006**, *440*, 163

[18] a) J. Berna, G. Bottari, D. A. Leigh, E. M. Perez, *Pure Appl. Chem*. **2007**, *79*, 39–54, b) M. R. Panman, B. H. Bakker, D. den Uyl, E. R. Kay, D. A. Leigh, W. J. Buma, A. M. Brouwer, J. A. J. Geenevasen, S. Woutersen, *Nat. Chem.* **2013**, *5*, 929–934.

[19] In contrast with the excellent templating ability of symmetrically dialkylsubstituted fumaramides reported by Leigh (reference 13), the employment of tetraalkylsubstitued ones notably drops down the rotaxanation yields.

[20] C. G. Collins, A. T. Johnson, R. D. Connell, R. A. Nelson, I. Murgu, A. G. Olivera, B. D. Smith, *New J. Chem*. **2014**, *38*, 3992–3998.

[21] For early examples of mechanically interlocked molecules containing this macrocycle see: a) C. A. Hunter, *J. Am. Chem. Soc.* **1992**, *114*, 5303-5311; b) F. Vögtle, S. Meier, R. Hoss, *Angew. Chem. Int. Ed. Engl.* **1992**, *31*, 1619-1622; c) F. Vögtle, M. Haendel, S. Meier, S. Ottens-Hildebrandt, F. Ott, T. Schmidt, *Liebigs Ann.* **1995**, 739–743; d) R. Jäger, F. Vögtle, *Angew. Chem. Int. Ed. Engl.* **1997**, *36*, 930-944.

[22] M. T. Rogers, J. C. Woodbrey, *J. Phys. Chem.* **1962**, *66*, 540–546.

[23] a) J. Berna, M. Alajarin, J. S. Martinez-Espin, L. Buriol, M. A. P. Martins, R.-A. Orenes, *Chem. Commun.* **2012**, *48*, 5677–5679; b) M. A. P. Martins, L. V. Rodrigues, A. R. Meyer, C. P. Frizzo, M. Hörner, N. Zanatta, H. G. Bonacorso, J. Berna, M. Alajarin, *Cryst. Growth Des.* **2017**, *17*, 5845–5857; c) T. Orlando, P. R. S. Salbego, G. C. Zimmer, A. B. Pagliari, C. R. Bender, L. V Rodrigues, H. G. Bonacorso, N. Zanatta, J. Berna, M. A. P. Martins, *Eur. J. Org. Chem.* **2018**, *2018*, 4978–4990; d)T. Orlando, P. R. S. Salbego, C. L. R. Taschetto, H. G. Bonacorso, N. Zanatta, M. Hoerner, M. A. P. Martins, *Cryst. Growth Des.* **2019**, DOI: 10.1021/acs.cgd.8b01560.

[24] A low conversion towards the free components was observed after 2 weeks at 373 K.

[25] P. Altoè, N. Haraszkiewicz, F. G. Gatti, P. G. Wiering, C. Frochot, A. M. Brouwer, G. Balkowski, D. Shaw, S. Woutersen, W. J. Buma, et al., *J. Am. Chem. Soc.* **2009**, *131*, 104–117.

[26] For other first-order photo-induced isomerization proccesses see: a) G. L. Duveneck, E. V. Sitzmann, K. B. Eisenthal, N. J. Turro, *J. Phys. Chem*. **1989**, *93***,** 7166-7170; b) K. S. Yim, G. G. Fuller, *Phys. Rev. E* **2003**, *67*, 041601; c) B. Kumar, K. A. Suresh, *Phys. Rev. E* **2009**, *80*, 021601.

[27] For examples of photocontrolled threading–dethreading processes see: a) K. Hirose, Y. Shiba, K. Ishibashi, Y. Doi, Y. Tobe, *Chem. Eur. J.* **2008**, *14*, 981-986; b) Y. Tokunaga, K. Akasaka, N. Hashimoto, S.Yamanaka, K. Hisada, Y. Shimomura, S. Kakuchi, *J. Org. Chem.* **2009**, *74*, 2374-2379; c) L. Zhu, D. Zhang, D. Qu, Q.Wang, X. Ma, H. Tian, *Chem. Commun.* **2010**, *46*, 2587-2589; d) T. Ogoshi, D. Yamafuji, T. Aoki, T. Yamagishi, *J. Org. Chem.* **2011**, *76*, 9497-9503; e) M. Baroncini, S. Silvi, M. Venturi, A. Credi, *Angew. Chem. Int. Ed.* **2012**, *51*, 4223-4226; f) A. Arduini, R. Bussolati, A. Credi, S. Monaco, A. Secchi, S. Silvi, M. Venturi, *Chem. - A Eur. J.* **2012**, *18*, 16203–16213; g) H. Li, C. Cheng, P. R. McGonigal, A. C. Fahrenbach, M. Frasconi, W.-G. Liu, Z. Zhu, Y. Zhao, C. Ke, J. Lei, et al., *J. Am. Chem. Soc.* **2013**, *135*, 18609–18620; h) V. Fasano, M. Baroncini, M. Moffa, D. Iandolo, A. Camposeo, A. Credi, D. Pisignano, *J. Am. Chem. Soc.* **2014**, *136*, 14245–14254; i) G. Tabacchi, S. Silvi, M. Venturi, A. Credi, E. Fois, *ChemPhysChem* **2016**, *17*, 1913–1919; j) L. Casimiro, J. Groppi, M. Baroncini, M. La Rosa, A. Credi, S. Silvi, *Photochem. Photobiol. Sci.* **2018**, *17*, 734–740.

[28] A. Kwiatkowski, B. Jędrzejewska, M. Józefowicz, I. Grela, B. Ośmiałowski, *RSC Adv*. **2018**, *8*, 23698–23710.

[29] A. Kinnell, T. Harman, M. Bingham, A. Berry, A. Nelson, *Tetrahedron* **2012**, *68*, 7719–7722.

[30] N. S. Simpkins, D. F. Weske, L. Male, S. J. Coles, M. B. Pitak, *Chem. Commun*. **2013**, *49*, 5010–5012